VOLUME 8 ISSUE 2 2022

ISSN 2454-3055

INTERNATIONAL JOURNAL OF ZOOLOGICAL INVESTIGATIONS

Forum for Biological and Environmental Sciences

Published by Saran Publications, India

International Journal of Zoological Investigations Vol. 8, No. 2, 435-443 (2022)

International Journal of Zoological Investigations
Contents available at Journals Home Page: www.ijzi.net
Editor-in-Chief: Prof. Ajai Kumar Srivastav
Published by: Saran Publications, Gorakhpur, India

ISSN: 2454-3055

In Vitro Mechanism of Hepatocellular Carcinoma (HepG-2) Inhibition by Activated Carbon Produced from *Musca acuminata* Fruit Peel

Vimala T.

Department of Plant Biology and Plant Biotechnology, Quaid-E-Millath Government college for Women (Autonomous), Anna Salai, Chennai 600 002, Tamil Nadu, India

Received: 4th August, 2022; **Accepted:** 16th September, 2022; **Published online:** 28th September, 2022

https://doi.org/10.33745/ijzi.2022.v08i02.053

Abstract: Cancer (CA) is global second cause of death and while drug discovery has advanced, new plant-derived medicines also need to be developed. Plant based medicinal products have many benefits as compared to the use of conventional chemical medications in minimizing the symptoms and side effects. The purpose of this study was to detect potential cytotoxicity (CYT) of activated carbon (AC) from *Musca acuminata* fruit peel. Significantly, the AC caused substantial increases in the synthesis of ROS, along with an attenuation of the mitochondrial (MTD) membrane potential and trigger caspase-3 activity activation in the HepG-2 cells. These findings showed that AC is a potential natural product source and provides prospects for developing new CA medicines.

Keywords: HepG-2 cells, MTT, DAPI/PI/EtBr staining**, C**omet assay

Citation: Vimala T. : *In vitro* mechanism of hepatocellular carcinoma (HepG-2) inhibition by activated carbon produced from *Musca acuminata* fruit peel. Intern. J. Zool. Invest. 8(2): 435-443, 2022.
https://doi.org/10.33745/ijzi.2022.v08i02.053

Introduction

Activated carbon (AC) is a high carbon (C) material treated to maximise the surface area. AC is often used to treat toxicity and toxic drugs (Qureshi *et al*., 2008; Chen *et al*., 2011; Foo and Hameed, 2012; Wu *et al*., 2013; Njoku *et al*., 2014; Njoku *et al*., 2015; Rahman and Chin, 2019). In one hour after ingesting poisonous chemicals, AC is the most effective(Lakshmi*et al*., 2018). The medications such as acetaminophen or paracetamol, lanoxin, digitoxin, tricycline antidepressants and phenobarbital have shown to be effective in both adults and children (Gupta *et al*., 2016; González-García, 2018). In the case of strong acids or bases, cyanides, biological solvents, ethanol, methanol, iron, lithium, among other substances, the AC is not effective (Nanda *et al*., 2016; Elanthamilan *et al*., 2019). Traditionally, AC is provided with laxatives to promote elimination of poisonous contents and increase carbon (C) resistance (Galan *et al*., 2018). There was no support from the EAPCCT for the combination of AC with a laxative substance (Zare *et al*., 2015; Wang *et al*., 2020). This can cause severe side effects, including hydration, electrolyte

disequilibria and low blood pressure (Spessato *et al*., 2019).

In several gastrointestinal conditions, including diarrhoea, gas and indigestion, AC has been studied. Research has shown that AC can help patients with chemotherapy-related diarrhoea (Rawal *et al*., 2018). AC may boost the effects of indigestion in combination with simethicone. In addition, AC can enhance bloating and stomach stress and avoid gas (Rahimian and Zarinabadi, 2020). Because of their adsorption, AC can also be used to treat hepatitis and renal disturbances (Gupta *et al*., 2021). AC by mouth can decrease cholesterol and decrease high bile acids (Dulyaseree *et al*., 2017). Light therapy can also be used to avoid jaundice (yellowing of the skin) of new-born babies (Beck *et al*., 2017). The drug delivery mechanism for improving therapy effectively and reducing side effects of the chemical agents has been examined with AC particles (Sharifpour *et al*., 2018). However, more research in this field is required. Keeping this in view, we described the mechanism for the acumination of *Musca acuminata* fruit peel mediated AC-cell inhibition in HepG-2 cells.

Materials and Methods

Sample collection and preparation of AC:

Sample collection and preparation of AC from *Musca acuminata* fruit peel was done according to the method of Ashok and Babu (2020).

MTT assay:

In order to assess the viability of HepG-2 and Vero cells as defined by Mosmann, MTT test method was followed (Mosmann, 1983). At 100% confluence, the HepG-2 cells were trypsinised and seeded in a 96 well platform at 7 x 10^3/well density. In a 37°C CO_2 incubator and 5% CO_2 the cells were incubated overnight for attachment in controlled, wet atmosphere. The solvent extract was exposed to various concentrations (25, 50, 75, 100 and 125 µg/ml) at 24 and 48 h after overnight incubation. The cells were filled with 50 µl MTT (5 mg/ml of stock) and incubated at 37°C for 3 h. The contents of the plate were discarded with a quick decantation at the end of the incubation cycle and the plate was dried overnight at room temperature (RT). The forming purple formazone crystals are solved by shaking at 400 rpm at RT in a thermo-shaker in 100 µl of DMSO for 15 min. A multimode microplate reader absorbed the strength of the produced colour at 570 nm. The cell viability (CV) percentage was determined in the following way:

Cell viability (%) = OD of experimental group x 100/ OD of control group

A pre-programmed MS-Excel prototype was used to measure the growth percentage, the percentage inhibition and 50 per cent growth inhibition (IC_{50}).

DAPI/PI/EtBr staining:

The nuclear stain, which has been treated to AC, and filtering appropriate for the Spector *et al.* (2001) method, has been performed to monitor the apoptotic (APT) morphology of cells under a fluorescence microscope (FLMICRO). At a confluence of 100 per cent the cells were trypsinised and sown on a cover slip (22 x 22 mm) set in the 6-well plate at a density of 1 x 10^5 cells/cover slip. The cells in a CO_2 incubator at a temperature of 37°C and 5% CO_2 were incubated overnight in a controlled humidified air to allow attachment. Cells were exposed, after overnight incubation, to IC_{50} levels of AC and incubated under controlled humidified atmosphere at 37°C and 5% CO_2 for 24 h. Cells were washed with 1X PBS at the end of 24 h (pH 7.4), 50 µl of PI was applied and incubated in dark at RT for 20 min. Cells were washed with 1X PBS (pH 7.4) at the end of the incubation, 50 µl DAPI/PI/EtBr were applied to cells and were washed immediately with 1X PBS. The cover slips have been stripped from the six-pad and put on a different cover slip (40 x 22 mm). The cover slips were presented in a 20 X magnification under a FLMICRO (Carl Zeiss) and cell images from various fields were taken.

Comet Assay/SCGE:

SCGE was conducted to record both the stability of DNA and DNA damage in the HepG-2 treatment

cells using the method of Singh *et al.* (1988). The slides were subsequently electrophored by horizon electrophoresis (ELP). The diaphragms have been separated from the solution to lysis and put in an ELP tank horizontally. The ELP tank was filled until the slides were submerged in the buffer and the slabs could stand in the tank for about 20 min with ELP at 0.8 Volts/cm for 15 min. The power supply was shut down and the slides were carefully removed and rinsed in a neutralisation buffer three times and dried carefully. On the gel a few drops of DAPI stain were applied and sealed with a covering slide. The stained DNA was analysed in cells using FLMICRO with an excitation filter of 365 nm and a barrier-filter of 435 nm at magnification 200X. The migrated DNA (Comet tail) long length was finally determined with the programme of the CASPLab (1.2.3 beta2).

Statistical Analysis:

Two-Way ANOVA analysed the data to evaluate the significance between the control and experimental groups. Statistical significance was taken into consideration at $p< 0.05$.

Results and Discussion

AC is a porous particle with a wide range of absorption. In the micro holes of AC, organic particles like drugs are easily placed on the basis of adsorption. AC as a transporter of CA drugs has unique features in their release of drugs. AC adsorbed chemicals usually through a physical contact and no covalent bond to make the adsorbed drugs readily disintegrate again into free pharmaceutical particles from the surface of AC. The drug accumulation of local entities in the body by the regulation of drug loading during preparation is thus highly beneficial. AC caused considerable damage to HepG-2 cells. The range of AC effects is 0.8~200 µg/ml, the released chemical molecules temporarily enclosed around the carrier particles, allowing the accumulation of medication in the area to be kept as high as possible, thereby possessing "local" characteristic. AC is smaller in diameter, the specified surface is larger and its adsorption is greater, enabling them to move medicines from administration to medicinal locations without major losses.

The AC had an impact tested by MTT method against HepG-2 CA cell lines at levels of 25, 50, 75, 100 and 125 µg/ml. A dose-dependent reduction in the CV was shown by tested AC. Another reduction in CYT has been seen in an increased duration of incubation. At these concentrations and exposure times, a concentration of 86.74 µg/ml AC at a time of 48 h was observed with a range of approximately 50% CYT inhibition. IC_{50} values in a AC treatment cells could not be achieved at 48 h (Figs, 1, 2).

In the FLMICRO experiments, significant improvements in nuclear morphology were found. Control and experimental groups are represented with staining DAPI on the percentage of HepG-2 cells showing apoptotic (APT) nuclear morphology. In our trial we have also found that HepG-2 cells have apoptosis (APA), which has resulted in 80% more DAPI stain than control. The potential mechanism of AC causes the MTD outer membrane's permeability to get triggered and release of the cytochrome-C during APA, causing caspase activation to orchestrate cell death due to the loss of the MTD function and the development of ROS. ROS overproduction may be linked to the imbalance in cell homeostasis, MTD disruption, and APA. Activating the MTD pathway for APA may be one of the major steps in APA generally linked to Caspase family protein recruitment, namely caspase-8 and/or caspase-3 (Fig. 3). A broad range of pathways have been identified as CA-protective effects of AC, including free radical scavenging, modification enzymes that cause or detoxify carcinogenic substances.

Cytomorphological observations of HepG-2 cells using DAPI staining were observed under FLMICRO. The control HepG-2 cells showed intact nuclei of uniform shape size with smooth edges whereas, IC_{50} concentration treated DAPI stained cells showed APT bodies which were indicated by red arrow. The white arrow indicated the disintegrated or cracking of HepG-2 cells and

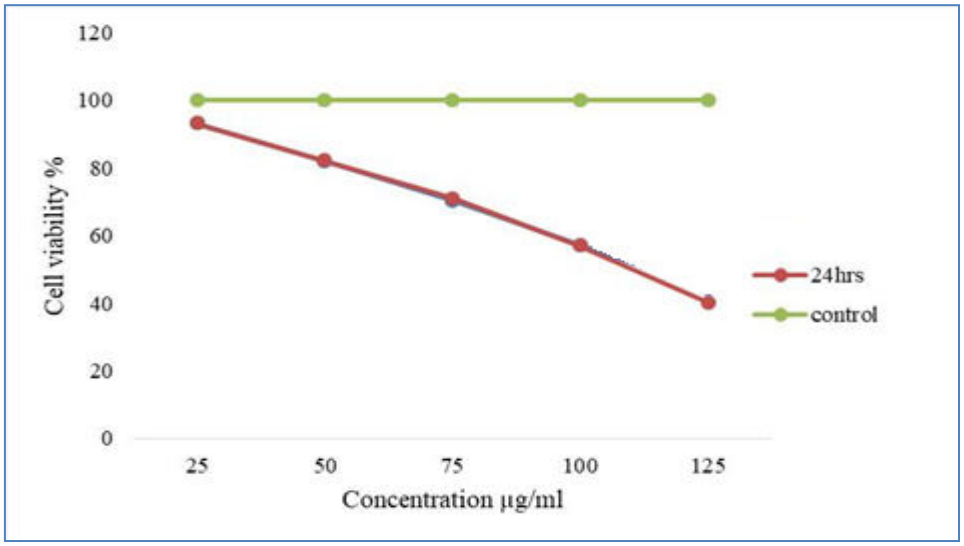

Fig. 1: Per CV of HepG-2 cell when treated for 24 h various concentration of AC.

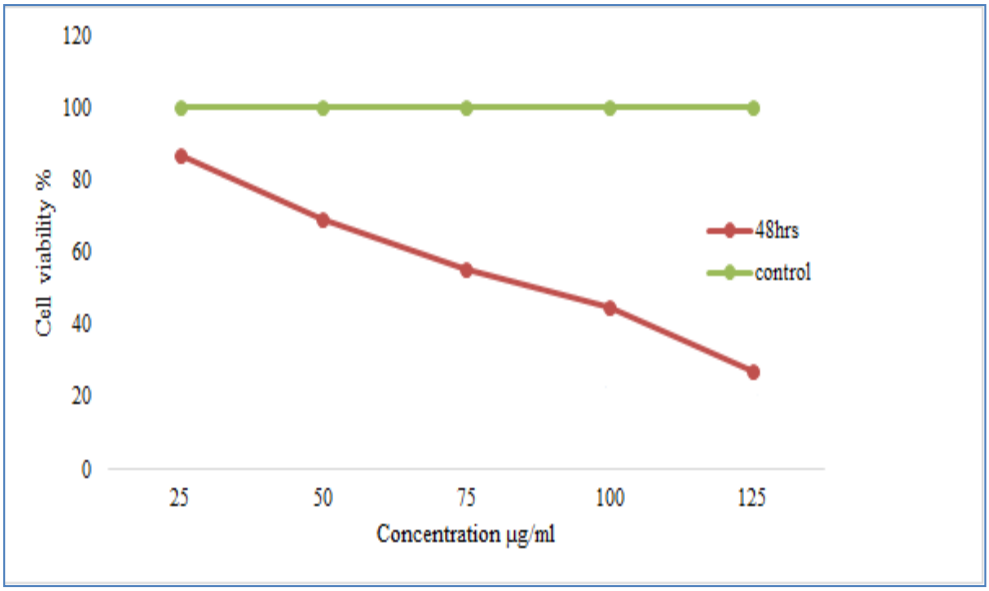

Fig. 2: Per CV of HepG-2 cell when treated for 48 h various concentration of AC.

overall the DAPI staining indicated that AC treated cells APT and disintegrated cells in a concentration depended manner. Yellow arrow indicated the reticular patterns of nuclear staining by PI. EtBr stained cells showed nuclear condensation, fragmentation and APT bodies which are marked by blue arrow in the IC_{50} concentration treated cells. Results of DAPI/PI/EtBr staining showed APT cells which were observed in the IC_{50} concentration treated cells when compared to control as shown in the Figure 4.

Comet assay or SCGE, a very sensitive assay, is used to detect and quantify even small amount of double strand DNA damage in individual cell. It is also known as single cell gel electrophoresis (SCGE). After removal of all the cytoplasmic

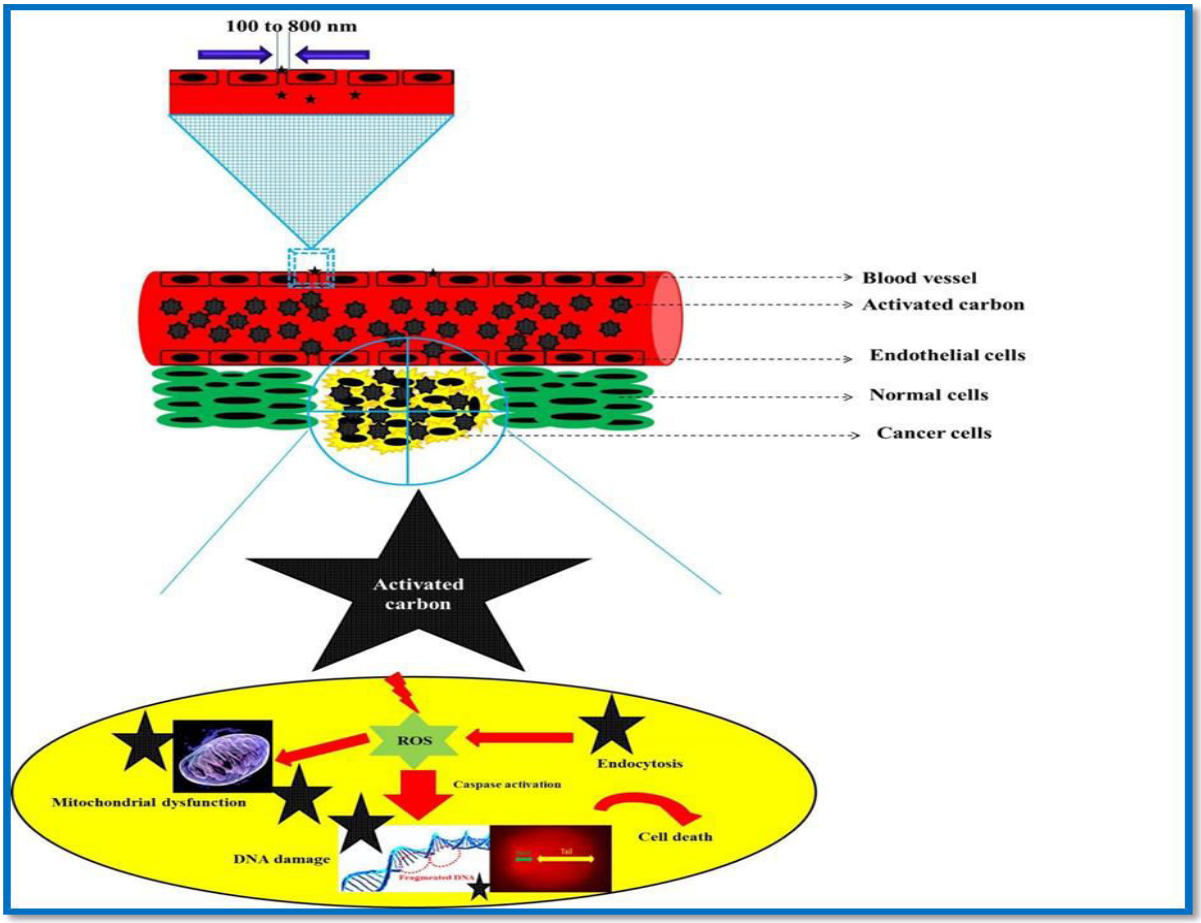

Fig. 3: Anticancer mechanism of activated carbon when treated with HepG-2 cells.

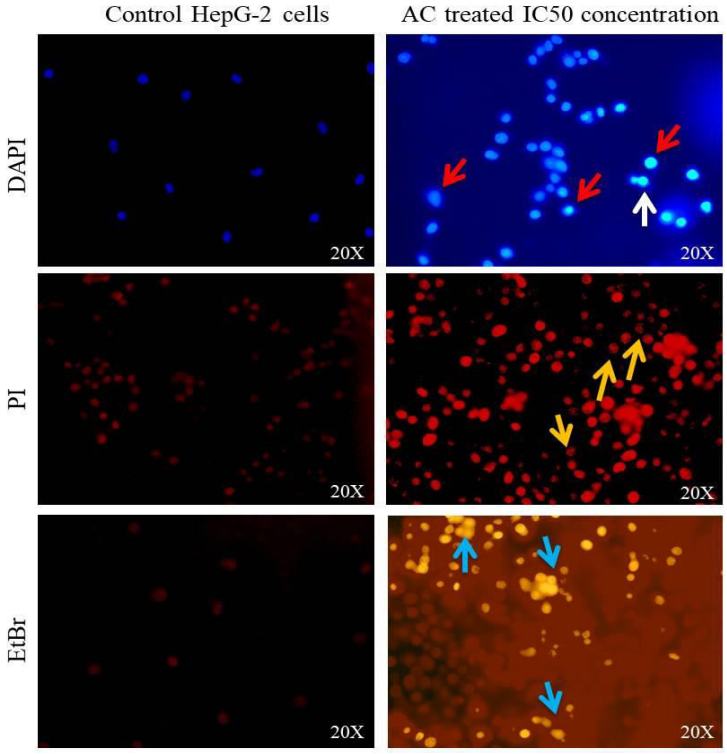

Fig. 4: DAPI/PI/EtBr staining of HepG-2 cells.

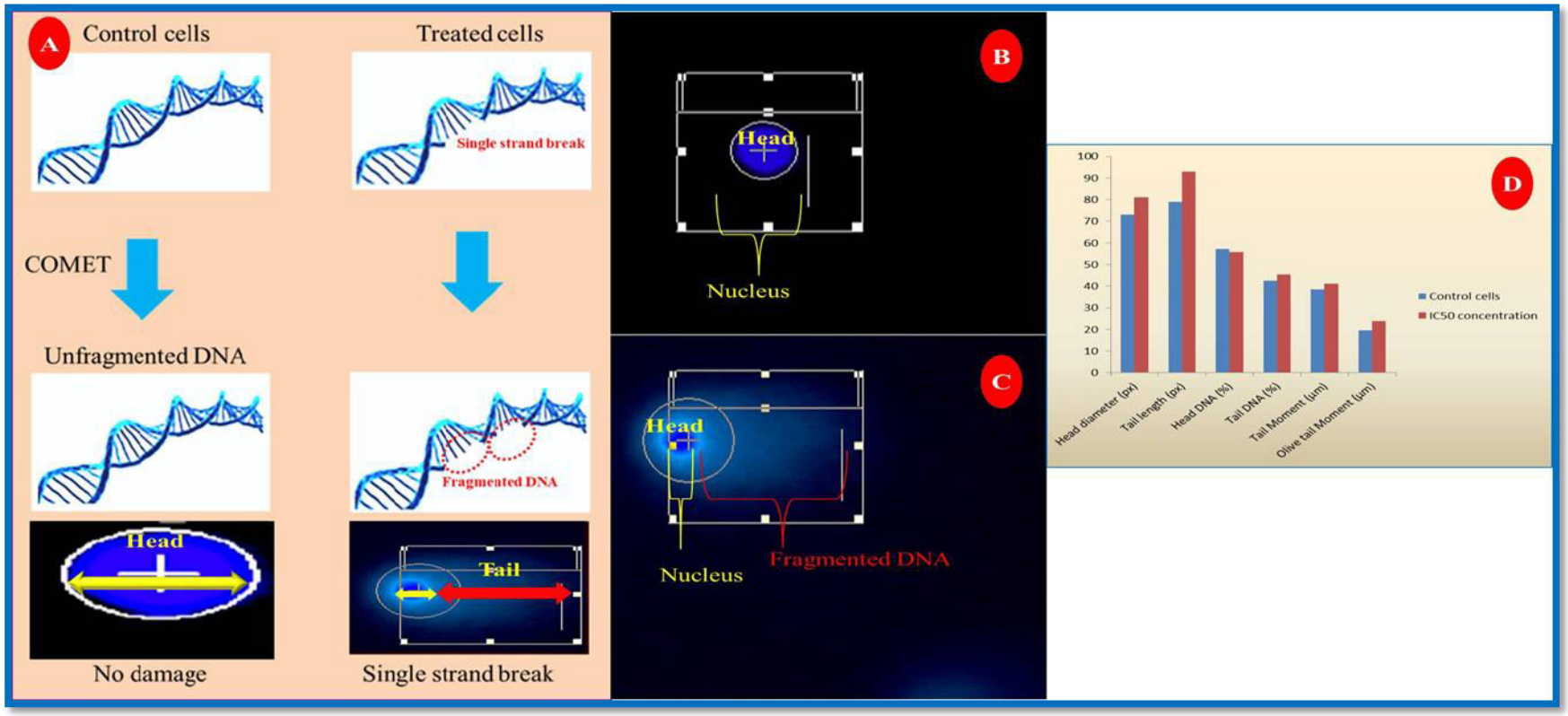

Fig. 5: A- SCGE mechanism, B- Control (untreated) HepG-2 cells where the DNA remains intact, C- IC_{50} concentration of AC and D- Quantitative DNA fragmentation analysis of HepG-2 cells when treated with 48 h IC_{50} concentration of AC to measure the SCGE head diameter, tail length, head DNA, tail DNA, tail moment and olive tail moment.

Table 1: CYT of AC used various CA cell lines

AC source	Incubation H	IC_{50}/GI_{50} value	Cell line name	Assays used	Ref
Coconut shell	24 h	20 mg/ml	H-1299	MTT assay, ROS assay and Hoechst/PI staining	(Chu *et al.*, 2013)
Cisplatin	Details not given in the paper		KU-1,HTB9	MTT assay and double layer soft agar colony assay	(Gotoh *et al.*, 1990)
Melittin	24 h	20 mg/ml	MCF-7and MDA-MB-231	XTT assay, LDH assay, ROS assay,MTD stability assay and Annexin-V/FITC staining	(Daniluk *et al.*, 2020)
Jack fruit seed and peel waste	Biological activity was not done				(Abid *et al.*, 2019)
Watermelon peel	Biological activity was not done				(Gin *et al.*, 2014)
Pomegranate, banana and kiwi fruit peels	Biological activity was not done				(Hashem *et al.*, 2016)
Red banana (*M. acumulata*) peel	24 h	120 µg/µl	MDA-MB-231	MTT assay	(Ashok and Babu, 2020)
Red banana (*M. acumulata*) peel	48 h		HepG-2	MTTassay, DAPI staining, Caspase-3 activity	Present study

proteins by cell lysing, in alkaline conditions, the DNA is allowed to unwind and then this unwound DNA is run in a gel by electrophoretic method. The damaged DNA migrates from negative to positive pole in the gel cast and form the tail part of the comet, whereas the intact DNA form the immobilizing head part of the comet. When stained with DAPI, the amount of blue fluoresce in the head, tail and tail length region indicated the level of damage in DNA as shown in Figure 5. Similar sensitivity towards various CA cells was observed for the CYT potential as shown in the Table 1.

Conclusion

The present study showed that AC can significantly inhibit HepG-2 cell formation, and the AC showed that it is likely via the ROS-mediated MTD pathway, followed by activated caspase-3 associated with APA cell death. These findings showed that AC is a potential source of valuable natural resources, and the new compound provides the possibility to create a new CA medicine after the complete therapeutic treatment of its APA activity. It is important to further investigate the mechanism behind the effectiveness of AC *in vivo.*

References

Abid MK, Ibrahim HB and Zulkifli SZ. (2019) Synthesis and characterization of biochar from peel and seed of jackfruit plant waste for the adsorption of copper metal ion from water. Res J Pharma Technol. 12(9): 4182-4188.

Ashok K and Babu M. (2020) Antiproliferative activity of activated carbon produced from Musa acuminate fruit peel against MDA-MB-231 cell line. Malaya J Matematik S(2): 4427-4429.

Beck RJ, Zhao Y, Fong H and Menkhaus TJ. (2017) Electrospun lignin carbon nanofiber membranes with large pores for highly efficient adsorptive water treatment applications. J Water Process Engineer. 16: 240-248.

Chen Y, Huang B, Huang M and Cai B. (2011) On the preparation and characterization of activated carbon from mangosteen shell. J Taiwan Inst Chem Engineers 42(5): 837-842.

Chu M, Peng J, Zhao J, Liang S, Shao Y and Wu Q. (2013) Laser light triggered-activated carbon nanosystem for cancer therapy. Biomaterials 34(7): 1820-1832.

Daniluk K, Kutwin M, Grodzik M, Wierzbicki M, Strojny B, Szczepaniak J, Bałaban J, Sosnowska M, Chwalibog A, Sawosz E and Jaworski S. (2019) Use of selected carbon nanoparticles as melittin carriers for MCF-7 and MDA-MB-231 human breast cancer cells. Materials (Basel) 13(1): 90.

Dulyaseree P, Fujishige M, Yoshida I, Toya Y, Banba Y, Tanaka YS, Aoyama T, Phonyiem M, Wongwieiyapan W, Takeuchi K and Endo M. (2017). Nitrogen-rich green leaves of papaya and *Coccinia grandis* as precursors of activated carbon and their electrochemical properties. RSC Adv. 7(67): 42064-42072.

Elanthamilan E, Sriram B, Rajkumar S, Dhaneshwaran C, Nagaraj N, Princy Merlin J, Vijayan A and Sea-Fue W. (2019) *Couroupita guianansis* dead flower derived porous activated carbon as efficient supercapacitor electrode material. Materials Res Bull. 112: 390-398.

Foo KY and Hameed BH. (2012) Factors affecting the carbon yield and adsorption capability of the mangosteen peel activated carbon prepared by microwave assisted K2CO3 activation. Chem Engineer J. 180: 66-74.

Galan CR, Silva MF, Mantovani D, Bergamasco R and Vieira MF. (2018) Green synthesis of copper oxide nanoparticles impregnated on activated carbon using *Moringa oleifera* leaves extract for the removal of nitrates from water. Canadian J Chem Engineer. 96(11): 2378-2386.

Gin WA, Jimoh A, Abdulkareem AS and Giwa A. (2014) Production of activated carbon from watermelon peel. Int J Sci Eng Res, 5: 66-71.

González-García P. (2018) Activated carbon from lignocellulosics precursors: A review of the synthesis methods, characterization techniques and applications. Renewable Sustainable Energy Rev. 82: 1393-1414.

Gotoh A, Maeda S, Takenaka A, Horio M, Gohji K and Kamidono S. (1990) A study on cisplatin adsorbed to activated carbon particles as a new drug delivery system and its anti-cancer effect against human bladder cancer cell lines. Jap J Urology 81(9): 1337-1342.

Gupta VK, Carrott PJM, Singh R, Chaudhary M and Kushwaha S. (2016) Cellulose: a review as natural, modified and activated carbon adsorbent. Bioresour Technol. 216: 1066-1076.

Gupta VK, Singh LP, Chaudhary M and Kushwaha S. (2021) A novel approach to develop activated carbon by an ingenious hydrothermal treatment methodology using *Phyllanthus emblica* fruit stone. J Cleaner Product. 288: 125643.

Hashem S, Fayza K, Foziah F and Mashael A. (2016) Comparative study on activated carbon prepared from various fruit peels. Int J Innov Res Sci Engineer Technol. 5(3): 2750-2759.

Lakshmi SD, Avti PK and Hegde G. (2018) Activated carbon nanoparticles from biowaste as new generation antimicrobial agents: A review. Nano-Struct Nano-Objects 16: 306-321.

Mosmann T. (1983) Rapid colorimetric assay for cellular growth and survival: Application to proliferation and cytotoxicity assays. J Immunol Methods 65(2): 55-63.

Nanda S, Dalai AK, Berruti F and Kozinski JA. (2016) Biochar as an exceptional bioresource for energy, agronomy, carbon sequestration, activated carbon and specialty materials. Waste Biomass Valor. 7(2): 201-235.

Njoku VO, Islam MA, Asif M and Hameed BH. (2014) Utilization of sky fruit husk agricultural waste to produce high quality activated carbon for the herbicide bentazon adsorption. Cheml Engineer J. 251: 183-191.

Njoku VO, Islam MA, Asif M and Hameed BH. (2015) Adsorption of 2, 4-dichlorophenoxyacetic acid by mesoporous activated carbon prepared from H3PO4-activated langsat empty fruit bunch. J Environ Managem. 154: 138-144.

Qureshi K, Bhatti I, Kazi R and Ansari AK. (2008) Physical and chemical analysis of activated carbon prepared from sugarcane bagasse and use for sugar decolorisation. Int J Chem Biomolec Engineer. 1(3): 145-149.

Rahman HA and Chin SX. (2019) Physical and chemical properties of the rice straw activated carbon produced from carbonization and KOH activation processes. Sains Malaysiana 48(2): 385-391.

Rahimian R and Zarinabadi S. (2020) A review of studies on the removal of methylene blue dye from industrial wastewater using activated carbon adsorbents made from almond bark. Progress Chem Biochem Res. 3(3): 251-268.

Rawal S, Joshi B and Kumar Y. (2018) Synthesis and characterization of activated carbon from the biomass of *Saccharum bengalense* for electrochemical supercapacitors. J Energy Storage 20: 418-426.

Sharifpour E, Ghaedi M, Nasiri Azad F, Dashtian K, Hadadi H and Purkait MK. (2018) Zinc oxide nanorod-loaded activated carbon for ultrasound-assisted adsorption of safranin O: Central composite design and genetic algorithm optimization. Appl Organometallic Chem. 32(2): e4099.

Singh NP, McCoy MT, Tice RR and Schneider EL. (1988) A simple technique for quantification of low levels of DNA damage in individual cells. Exp Cell Res. 175(1): 184-191.

Spector DL, Auman RD and Leiward LA. (2001) Cell culture analysis: Apoptosis analysis. In: Cell - A Laboratory Manual, (eds.) Coldspring Harbour Laboratory Press, New York, USA, pp. 6-15.

Spessato L, Bedin KC, Cazetta AL, Souza IPAF, Duarte VA, Crespo LHS, Silva MC, Pontes RM and Almeida VC. (2019) KOH-super activated carbon from biomass waste: Insights into the paracetamol adsorption mechanism and thermal regeneration cycles. J Hazard Mater. 371: 499-505.

Wang S, Nam H and Nam H. (2020) Preparation of activated carbon from peanut shell with KOH activation and its application for H2S adsorption in confined space. J Environ Chem Engineer. 8(2): 103683.

Wu M, Guo Q and Fu G. (2013) Preparation and characteristics of medicinal activated carbon powders by CO2 activation of peanut shells. Powder Technol. 247: 188-196.

Zare K, Gupta VK, Moradi O, Makhlouf ASH, Sillanpää M, Nadagouda MN, Sadegh H, Shahryari-ghoshekandi R, Pal A, Wang Z, Tyagi I and Kazemi M. (2015) A comparative study on the basis of adsorption capacity between CNTs and activated carbon as adsorbents for removal of noxious synthetic dyes: a review. J Nanostruct Chem. 5(2): 227-236.